



MODELING DAHR EL BAIDAR SLOPE WITH AN INTEGRATED GEO-ASSESSMENT

Muhsin RAHHAL¹, Dalia YOUSSEF ABDEL MASSIH², Jacques HARB³, Fadi HAGE-CHEHADE⁴, Chadi ABDALLAH⁵, Layla KHALAF-KEYROUZ⁶, Grace ABOU-JAOUDE⁷, Elsy IBRAHİM⁸, Georges NASR⁹ and Alexandre SURSOCK¹⁰.

ABSTRACT

The slope of Dahr El Baidar located on the central mountain of Lebanon hosts a section of the Arab Highway that is under construction to connect Beirut to neighboring Arab countries. This slope has experienced failures and seismic movements, yet most involved geotechnical companies have investigated the slope with classical geotechnical procedures. In this paper, the slope analysis is an integrated approach to identify the principal causes of failure. Thus, the study includes geological, geophysical and geotechnical soil characterization of the designated area. The geological analysis reveals the presence of faults in the vicinity, in addition to a layer of weak clay at the surface. The geotechnical investigation is based on the interpretation of several boreholes for which quality assessment is carried out using in-situ sampling and lab tests. Geophysical tests are performed using ambient noise vibration technique with the Horizontal to Vertical Spectrum Ratio HVSR method, in order to reveal the resonant frequency and thickness of the subgrade material. The above data is used towards a better understanding of the cause and occurrence of the failing zone. It is suspected that the main triggering factor is water. Further analysis will be carried out to evaluate the effect of an earthquake loading.

This work is part of the assessment and prediction of the behavior of various critical slopes in Lebanon carried by RUMMARE, a Research Unit on Mass Movement hazard Assessment and Risk Evaluation grouping researchers from major universities and research centers in Lebanon.

¹ Saint Joseph University, ESIB, CLERC, Beirut, Lebanon, muhsin.rahal@usj.edu.lb

² Notre Dame University Louaize, Lebanon, dabdelmassih@ndu.edu.lb

³ Notre Dame University Louaize, Lebanon, jharb@ndu.edu.lb

⁴ Lebanese University, Modeling Center, Doctoral School of Sciences and Technology, Beirut, Lebanon, fhagechade@ul.edu.lb

⁵ Lebanese National Council For Scientific Research, Remote Sensing Center, Lebanon, chadi@cnrs.edu.lb

⁶ Notre Dame University Louaize, Lebanon, lkhalaf@ndu.edu.lb

⁷ Lebanese American University, Beirut, Lebanon, grace.aboujaoude@lau.edu.lb

⁸ Notre Dame University Louaize, Lebanon, eibrahim@ndu.edu.lb

⁹ Lebanese University, Faculty of Engineering II, Roumieh, Lebanon, george.j.nasr@gmail.com

¹⁰ Lebanese National Council For Scientific Research, Geophysical Center, Lebanon, asursock@cnrs.edu.lb

INTRODUCTION

The Lebanese territory is featured by two mountainous chains, one on the eastern border with Syria and the other located in the middle, bordering east a coastal zone with the eastern Mediterranean Sea. They both bound the Bekaa valley, a fertile plain of alluvial soil. This complex topography presents challenging geological heterogeneities. It is also the location of three microclimates ranging from cold mountainous to continental and tempered humid coastal one a feature appealing to population density.

Apart from the eastern mountains, the area is densely populated leading to scarcity of land and rocketing price. Green space is wildly invaded by construction, leading to insufficient infrastructural projects. Even steep slopes are not stopping owners from building, in spite of the geotechnical elevated risks.

The eastern Mediterranean is known for a relatively moderate to high seismicity. Historical events showed a wide range of destruction due to earthquakes. The georisk characteristics coupled with intense construction justified by a real estate booming for the past 15 years induced researchers to investigate alternative methods of addressing foundation soils. Geophysical investigation can be merged with geotechnical classical approaches. Opportunities arise to use both methods in the event of failure such as slope instability, due to the presence of previous soil studies. In this paper, the case of Dahr El Baidar slope stability is illustrated and presented below.

SITE LOCATION AND CHARACTERISATION

Dahr El Baidar is located at 33°48'18"N 35°45'42"E (see Fig.1) on the slope of a mountainous area in the center of Lebanon. The site is hosting a portion of the "Pan Arab Highway"(see Fig.1 and Fig.2), a main road connecting the coastal zone to the Bekaa valley reaching east the Lebanese Syrian border. It is a vital infrastructure project that has been delayed at several instances due to slope stability problems. In spite of the numerous geotechnical investigations, this particular site still presents a challenge to designers and contractors as a result of its complexity.

Aiming to study the most probable cause of the slopes failure in this region, an experimental campaign was carried out. Eight geotechnical boreholes were conducted (Noted AB in Fig.1) as well as 23 geophysical ambient noise measurements (Noted Pt in Fig.1).

GEOLOGICAL ENVIRONMENT

The major tectonic features in Lebanon surrounding Dahr El-Baidar are (i) the Yammouneh Fault which is part of the Levantine fault extending from the Aquaba golf, passing by the Jordan valley and Dead Sea, Bekaa valley and north to the Taurus Zagros Mountains of Turkey; (ii) the Roum Fault which is a branching of the Levantine Tammouneh fault starting from Roum village South, and extending North-West up to the capital Beirut and (iii) the Occidental flexures parallel to the Yammouneh fault regrouping a multitude of minor faults with variable activities.

The Dahr el-Baydar slope is located on the center of Mount Lebanon, located in a zone distanced around 5 kilometers from the Yammouneh fault, 31 km from the coastal line and 26 km from the Roum fault. The area is characterized by a significant tectonic activity.

The plateau of Dahr El Baidar rock formation range from the lower to middle cretaceous (C_1 to C_3 respectively); around 6 km west of the Yammouneh fault. This area is positioned in a subducted zone, bounded by two minor East-West faults and highly scattered by other minor faults connected to the Yammouneh fault. The predominant ones are (i) The Kab-Elias Wadi El-Delm fault, 3.5 km south in the East-West direction, limiting the Jurassic plateau of Jabal El Barouk against the depression of Dahr El Baidar, (ii) a portion of the Yammouneh fault extending around 6 km oriented NNE-SSW to the East, and (iii) a 2 km stretch of Jabal El Roueiss fault in the E-W orientation. The system of faults is active however, their individual activity is difficult to trace due to the lack of instrumentation on site and close vicinity.

The structural geology is characterized by sub horizontal layers or slightly inclined to the right around 10° North West. The regional litho-stratigraphy extends from the Jurassic to the upper Albien as defined from below up:

- Grès de Base C₁: around 200m made up of sand and red-brown sandstones formed from quartz grains with cementations of clayey-sand lignites. Volcanic turf from basaltic origins is shown.
- Lower Aptien C_{2a} : around 120 m where sandstones become clayey sand and darkoolitic limestone
- Upper Aptien C_{2b} : around 90m formed of limestone layers at the base, followed by a series of clayey sandstones, lignites are present
- Albien C₃: Limestone layers alternating with greenish marl.
- Jurassic J₆: Keserwan Limestone, blue massive limestone, bluish in color, slightly karstified.

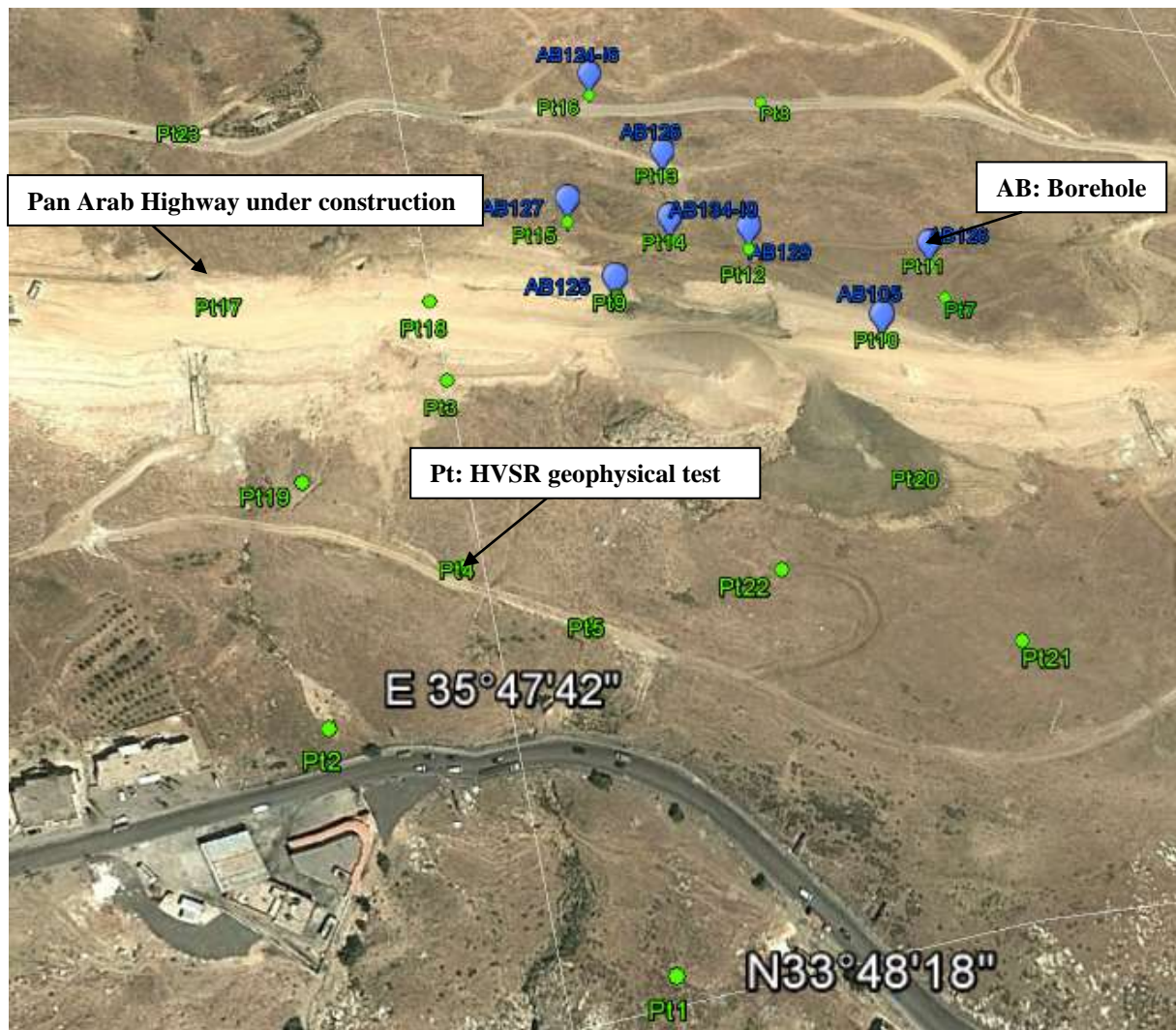


Figure 1. Site Location (from Google earth) including the location of the Pan Arab Highway, HVSR tests and Boreholes.



Figure 2. The Pan Arab Highway under construction

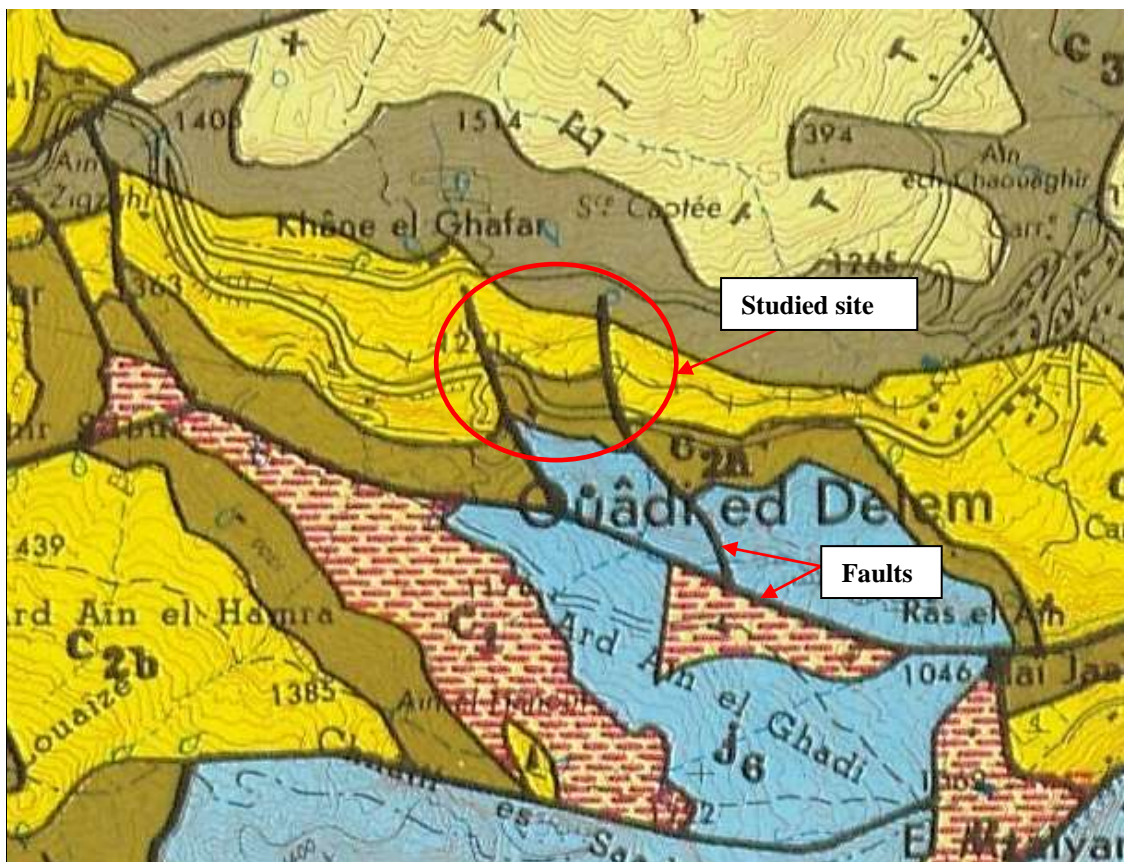


Figure 3: Geological map of the studied site including the faults (Dubertret, L., 1945)

GEOTECHNICAL INVESTIGATION

In order to understand soil behaviour before, during and after the triggering of a landslide process, a very important issue is to examine soil geotechnical properties, and define the different existing soil layers within a slope. In the portion of the Pan Arab Highway being analysed, boreholes and all available soil data are deeply investigated to establish typical cuts along the observed crack line (Surface failure line). This analysis should help in understanding the triggering factors behind the observed slope instabilities. Figure 4 gives the location of the 7 analysed boreholes, as well as the sections A-A, B-B, C-C and D-D considered. Table 1 shows the location (coordinates, and altitude) of the different boreholes, as well as the depth reached and the date of testing. Table 2 provides information on each and every section as far as the coordinates of two points on each concerned section. All geotechnical properties as well as soil layers in the 4 sections are discussed in Figures 5, 6, 7 and 8.

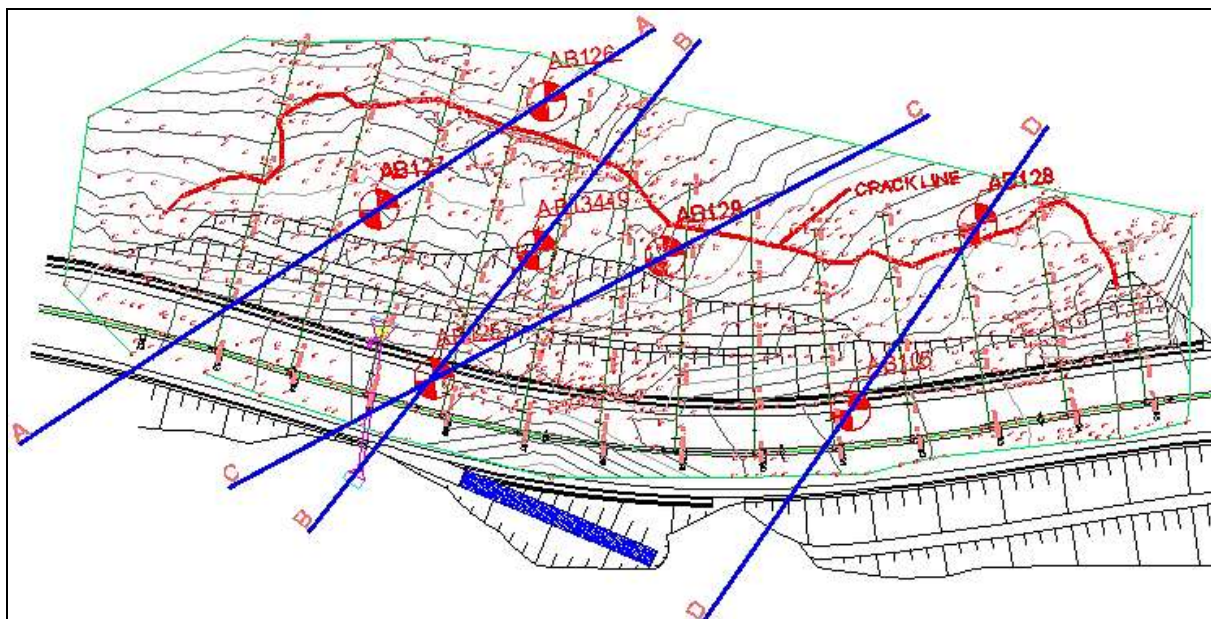


Figure 4: Part of the Pan Arab Highway that underwent failure (crack-line) with the boreholes and the 4 sections A-A, B-B, C-C; D-D.

Table 1: Borehole Local Coordinates, Altitude, Depth reached and date realized.

Borehole	Local X	Local Y	Altitude above sea level (m)	Depth (m)	Date of Borehole
AB 105	-310399.52	-38422.13	1313.83	16	06/2010
AB 125	-310528.57	-38393.22	1322.18	20	07/2011
AB 126	-310482.90	-38314.05	1350.21	35	07/2011
AB 127	-310539.69	-38340.86	1338.52	30	07/2011
AB 128	-310352.51	-38369.13	1321.38	30	07/2011
AB 129	-310452.10	-38366.86	1333.07	30	07/2011
AB 134	-310491.86	-38360.21	1337.96	20	07/2011

Table 2: Coordinates of the two points used to define sections A-A, B-B, C-C and D-D:

Section	First point			Second point		
	Longitude	Latitude	Altitude	Longitude	Latitude	Altitude
A – A	35.7964	33.8085	1350.21	35.7958	33.8082	1338.52
B – B	35.7959	33.8078	1322.18	35.7963	33.8081	1337.96
C – C	35.7959	33.8078	1322.18	35.7967	33.8080	1333.07
D – D	35.7973	33.8075	1313.83	35.7978	33.8080	1321.38

In section A-A (Figure 5), the water table is deep and the following soil layers and properties are considered: At the surface, a marly fill is found next to the crack line. Then, cemented brown sand with presence of clay of low plasticity (CL) is identified with the following shear strength properties (an effective cohesion $c' = 44\text{kPa}$ and an effective friction angle $\phi' = 17^\circ$, a plasticity index of $PI=18\%$, and a Standard Penetration Test number $SPT N = 11$). Below, a clayey sand is found ($c' = 26\text{kPa}$ and $\phi' = 25.8^\circ$, $PI=14\%$, and $SPT N = 21$). A greyish marl and limestone (with pressuremeter results giving Limit Pressure $P_1 = 2.7\text{ MPa}$ and Menard elastic modulus $E_m = 43.5\text{ MPa}$) interbedded between two clay layers with different properties: the upper clay has a $P_1 = 420\text{ kPa}$, and $E_m = 3.3\text{MPa}$, while the lower clay has a $P_1 = 2.8\text{ MPa}$ and $E_m = 163\text{ MPa}$. In depth, marl with different colors (brown, grey and beige) was found with $P_1 = 3.9\text{ MPa}$ and $E_m = 121\text{ MPa}$. Below, Marly Sandstone is identified.

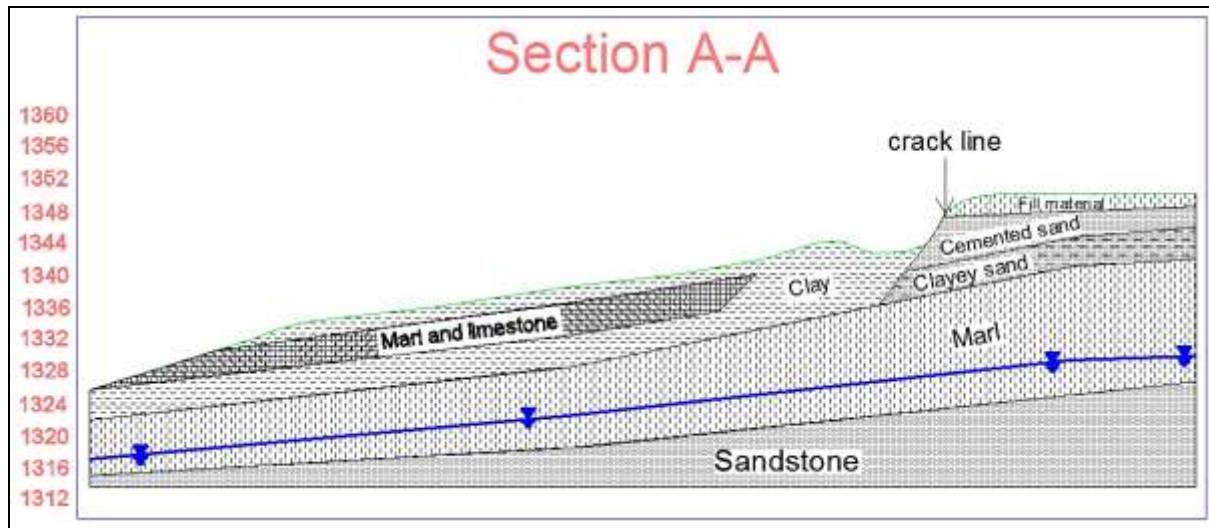


Figure 5: Soil Layers in section A – A

In section B-B (Figure 6), the following layers and properties are well-thought-out. At the surface, a clayey silty yellowish and brown loose sand is identified at the crack line with $c' = 23\text{kPa}$, $\phi' = 23^\circ$ and $SPT: N = 6$. Below the highway, a limestone loose fill is found with $SPT N = 9$. Below, a clayey marl CL yellow to beige is defined with $c' = 32\text{kPa}$, $\phi' = 18^\circ$ and $SPT N = 11$. Then, a low permeability layer CL-ML (silty clay of low plasticity) with a plasticity index of 6.6% is defined over a fractured limestone. Deeper, a layer of marl and limestone is identified with these properties ($c' = 28\text{kPa}$, $\phi' = 24^\circ$ and $PI=14\%$). Finally, sand ($SPT N=28$) and sandstone is found at the base. Water table is located at 4m below the highway.

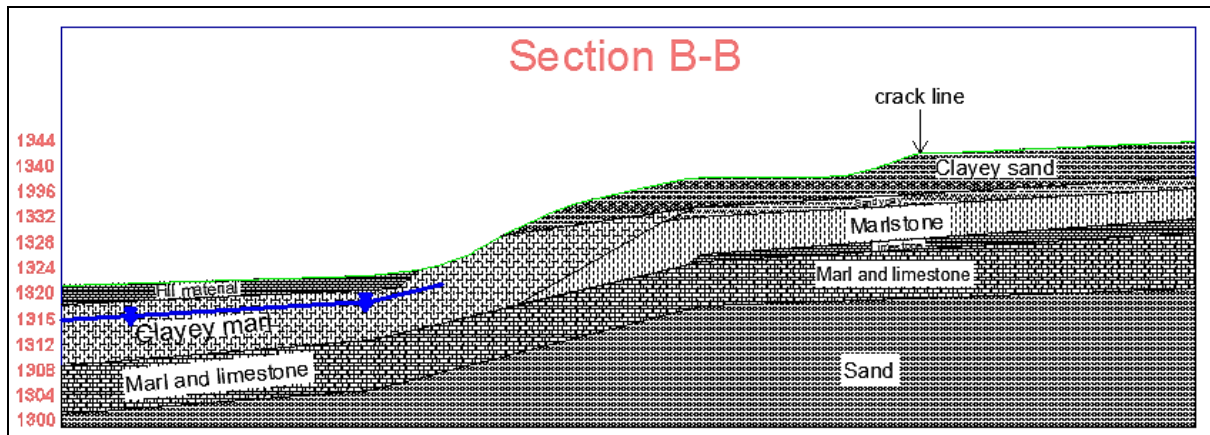


Figure 6: Soil Layers in section B – B

In section C-C, water table is 4 meters below the highway, as defined in Figure 7. At the surface, different layers of soft marl are identified (CL or CL-ML, a plasticity index of 10 and SPT N=9) interbedded with limestone. Under the highway, a calcareous fill with beige marl (SPT N=9) is found. Then a soft yellowish clayey marl CL is identified with $c' = 32\text{kPa}$ and $\phi' = 18^\circ$. Deeper, beige marl and limestone are found again with the following properties in the marl: $c' = 28\text{kPa}$, $\phi' = 24^\circ$, and a plasticity index between 10% and 17%. The deepest layer identified is sand and sandstone with an SPT N=23.

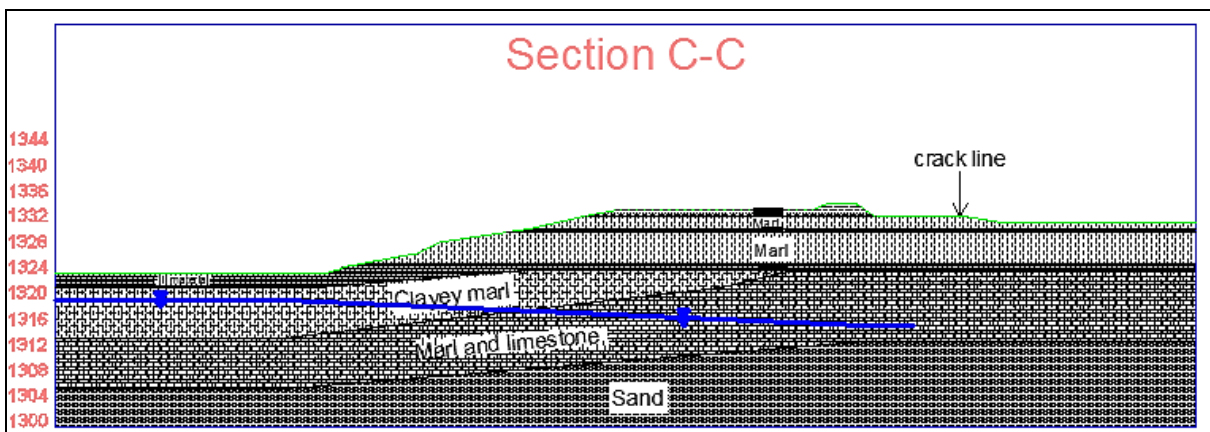


Figure 7: Soil Layers in section C – C

In section D-D, water is relatively deep in all the section as shown in Figure 8, at the interface between marl and limestone and clayey sand. The crack line goes through the fill material which is mostly clayey sand with clay lenses CL having the following properties: $c' = 29\text{ kPa}$, $\phi' = 19^\circ$, a plasticity index of 10, $PI = 2.1\text{ MPa}$ and $E_m = 25.6\text{ MPa}$. Under the highway, clay is found with $c' = 24\text{ kPa}$, $\phi' = 24^\circ$, and a plasticity index of 12. Underneath the clay layer, another clay CL and limestone layer is identified with $c' = 40\text{ kPa}$, $\phi' = 15^\circ$, and SPT N=36. It is followed by a marly CL limestone with $PI = 3.8\text{ MPa}$, and $E_m = 62\text{ MPa}$, resting on a weaker marl ($PI = 1.5\text{ MPa}$ and $E_m = 13\text{ MPa}$). Then, clayey sand is identified with a plasticity index of 9. And finally, the deepest layer defined is fractured limestone adjacent to sand with pressuremeter properties as follows: $PI = 2.3\text{MPa}$, and $E_m = 24\text{ MPa}$).

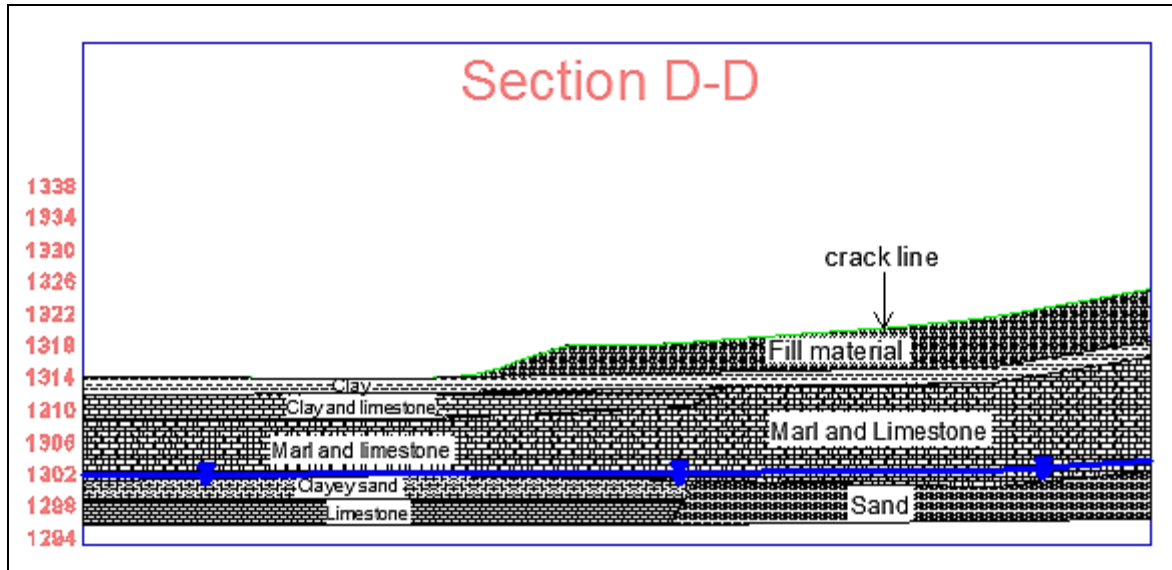


Figure 8: Soil Layers in cut D – D

GEOPHYSICAL INVESTIGATION

The H/V method (known also as the HVSR technique) was originally suggested by Nogoshi & Igarashi (1971), and wide-spread by Nakamura (1989). It aims at estimating the ratio between the horizontal and vertical spectrum components of seismic ambient noise registered at the surface of a material. It has been proven numerically and experimentally that the peak of the H/V spectral ratio gives the fundamental resonance frequency (or period) of the material (or site) (see for instance Field and Jacob, 1995; Bonnefoy-Claudet et al., 2006; Haghshenas et al., 2008). This method is thus frequently utilized to rapidly estimate the natural frequency of a soil (or any other system) as well as the depth to bedrock or the limits between soft and stiff horizontal soil layers based on the following eq. 1:

$$f_0 = \frac{V_s}{4H} \quad (1)$$

Where

f_0 is the fundamental soil frequency

H is the depth of the soft layer to the bedrock

V_s is shear wave velocity of the softer layer

Twenty three H/V tests were performed on Dahr El Baidar site as shown previously on the fig. 1 using Lennartz-5s velocimeters (cut-off period of 5 seconds) connected to a CitySharkTM acquisition unit (Chatelain et al., 2000) with a 200 Hz sampling rate. Geopsy software (<http://www.geopsy.org>; Wathelet et al. 2008) was used to compute the H/V spectral ratios of the registered ambient noise at several locations. A b-value of 40 was used in the smoothing procedure of Konno & Ohmachi (1998) for the computed Fourier amplitude spectra. The two horizontal components (North-South and East-West) were then combined by computing the quadratic mean and H/V ratios computed by averaging the H/V ratios obtained on individual 10s windows.

Due to the site heterogeneity, no clear peak frequency was observed. However, a dominant frequency f_0 between 9 and 15Hz (See fig. 9) was noticed on most of the H/V measurements. The estimated f_0 from the HVSR measurements at the borehole locations with the corresponding depth D of soft soil to the stiffer layer are reported on Table 3. If equation 1 is used for values of Table 3, the values of the shear wave velocity will range from 100m/s to 400m/s. However, the use of eq.1 for the case of a slope ground is questionable. In order to check the accuracy of the results, MASW test is found to be necessary.

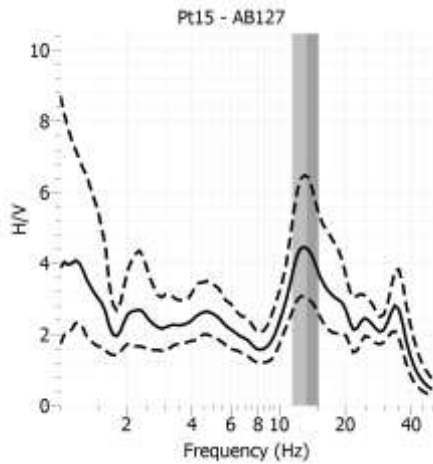


Figure 9: H/V spectrum of Pt15 (AB127)

Table 3: f_0 versus D

HVSR tests	Borehole	f_0 (Hz)	D (m)
Pt9	AB125	12.52	2
Pt10	AB105	12.45	4
Pt11	AB128	12.77	8
Pt12	AB129	12.7	4
Pt13	AB126	13	9
Pt14	AB134	9.5	6
Pt15	AB127	13	2

FAILURE ANALYSIS

As it could be seen, the geotechnical investigation is quite important and many soil layers are defined. But the soil properties cannot explain alone the cause of the slope instabilities. To prove that, a slope stability analysis was performed using the finite element software PLAXIS on sections A-A and B-B based on the strength reduction technique where the safety factor is defined as follows:

$$FS = \frac{S_{\text{max available}}}{S_{\text{needed for equilibrium}}} \quad (2)$$

Where S represents the shear strength. The ratio of the true strength to the computed minimum strength required for equilibrium is the safety factor that is conventionally used in soil mechanics. By using the standard Mohr Coulomb criterion, the safety factor will be defined as:

$$FS = \frac{c}{c_r} = \frac{\tan \varphi}{\tan \varphi_r} \quad (3)$$

Where c and φ are the input strength parameters and c_r and φ_r are the reduced maximum shear strength parameters needed for equilibrium.

The safety factors obtained using Plaxis was found greater than 2 for both sections. However, the most probable failure surface was found to be at the interface between the clay layer and the marl layer. (See Fig.10)

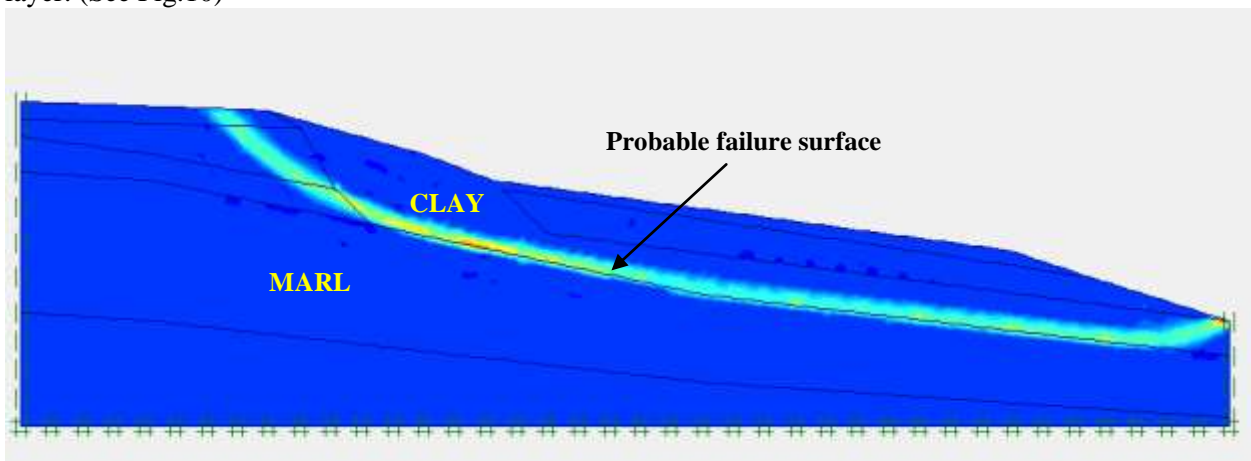


Figure 10: Incremental Shear strain shadings showing the most probable failure surface located at the Clay-Marl interface for section A-A.

The properties shown and used in the analysis are not the ones measured during the period of failure, and we do not know exactly what the soil properties were at the time of the triggering of the slide. It is suspected at this stage that the main triggering factor was water. As we know, soils properties are affected by the presence of water especially the soils with very high fine contents (marl and clay). These soils lose an important part of their cohesion in the presence of water, reducing at the same time their shear strength. As for the failure surface is concerned, it is thought that it was induced at the interface of two materials with different rigidities, or within a soft material itself. All the scenarios within the different sections will be examined later to determine the failure surfaces and assess the triggering agents responsible of the slope instabilities.

Another possible triggering agent that needs to be studied is earthquake induced ground shaking, which is a very recurrent cause of slope instabilities. Geotechnical soil properties are affected by undrained loading; shear deformations generated in the slope will without any doubt reduce soil rigidity. A relation between the yield acceleration, the soil cohesion and the slope angle has already been established for other cases (Rahhal, 2014). An essential aspect to investigate is the relation between the dynamic factor of safety and soil mechanical properties. Furthermore, the stability of the slope under seismic loading will be assessed through a sensitivity analysis covering both the dynamic soil properties as well as the earthquake parameters. The role of the shear wave velocity V_s , the small strain shear modulus G_{max} as well as the degradation of these two properties with the induced shear strains will be analyzed in order to appreciate the slopes response to earthquake loading.

CONCLUSIONS

In this paper, an integrated geo-assessment was conducted on Dahr El Baidar slope – Lebanon that hosts a section of the Arab Highway under construction. The geological analysis has shown the presence of faults in the vicinity as well as a layer of weak clay at the surface. The geotechnical investigation was based on the interpretation of 7 boreholes. Geophysical tests are performed using ambient noise vibration technique based on the HVSR method to estimate the resonant frequency. Since the analysis of soil data based on the cross sections have shown a high fine percent, and since fine soils lose an important part of their cohesion in the presence of water, due to the reduction of their shear strength. It was suspected that the failure was probably induced at the interface of two materials with different rigidities or within a soft material itself. Further analysis is needed to evaluate the slope failure under earthquake loading.

Additional geophysical tests are also necessary to better estimate the dynamic properties of the soil. All the scenarios of the different cross sections will be examined later to determine the static and dynamic failure surfaces and to examine the triggering factors behind the slope instabilities.

ACKNOWLEDGMENT

The authors of the paper would like to thank the National Council for Scientific Research in Lebanon (NCSRL) for funding the RUMMARE research unit. They would like to thank also the IS-Terre Laboratory of the University of Grenoble - France for making the Velocimeter and CityShark Machine available to the Research Unit. Another thank you goes to the Graduate students Akram Ghossoub, Anthony Fayad and Therèse Matar.

REFERENCES

- Bonnefoy-Claudet, S., Cornou, C., Bard P.Y., Cotton, F., Moczo, P., Kristek, J. and Fäh, D. (2006). "H/V ratio: a tool for site effects evaluation. Results from 1D noise simulations." *Geophysical Journal International*, 167(2): 827-837. doi: 10.1111/j.1365-246X.2006.03154.x
- Chatelain J.L., Guéguen P., Guillier B., Fréchet J., Bondoux F., Sarrault J., Sulpice P., and Neuville J.M. (2000). "CityShark : A user-friendly instrument dedicated to ambient noise (microtremor) recording for site and building response studies." *Seismological Research Letters*, 71(6), 698-703.

- Dubertret, L., (1945). "Geological Map of Zahlé, 1/50,000." Ministry of National Defence-Geography Department, Lebanon.
- Field E.H., and Jacob K.H. (1995). "A comparison and test of various site-response estimation techniques, including three that are not reference-site dependent." *Bulletin of the Seismological Society of America*, 85(4), 1127-1143.
- Haghshenas, E., P.-Y. Bard, N. Theodulidis and SESAME WP04 Team, (2008). "Empirical evaluation of microtremor H/V spectral ratio." *Bulletin of Earthquake Engineering*, 6-1, pp. 75-108.
- Konno, K. and T. Ohmachi, (1998). "Ground-motion characteristics estimated from spectral ratio between horizontal and vertical components of microtremor." *Bulletin of the Seismological Society of America*, 88(1), 228-241.
- Nakamura, Y., (1989). "A method for dynamic characteristics estimation of subsurface using microtremors on the ground surface." *Quarterly reports of the Railway*, Technical Research Institute, Tokyo, 30, 25–33.
- Nogoshi M. and Igarashi T. (1971). "On the amplitude characteristics of microtremor." *Journal of seismological Society of Japan*, 24, 26-40.
- Rahhal, M.E. (2014). "The factor of safety in slopes under earthquake loading." *Geo-Congress 2014, Geotechnical Special Publication 234*, ASCE, 1274-1283.
- Wathelet, M., D. Jongmans, M. Ohrnberger, and S. Bonnefoy-Claudet (2008). "Array performances for ambient vibrations on a shallow structure and consequences over Vs inversion." *Journal of Seismology*, 12, 1-19.